AUT Journal of Modeling and Simulation

AUT J. Model. Simul., 51(2) (2019) 139-152
DOI: 10.22060/miscj.2019.15315.5130

Modeling and Neuro-fuzzy Controller Design of a Wind Turbine in Full-load Region Based on Operational Data

V. Fazlollahi[1], M. Taghizadeh[1,*], F.A. Shirazi[2]

[1] Faculty of Mechanical and Energy Engineering, Shahid Beheshti University, Tehran, Iran.
[2] School of Mechanical Engineering, University of Tehran, Tehran, Iran

ABSTRACT: In this paper, dynamic modeling of a Vestas 660 kW wind turbine and its validation are performed based on operational data extracted from Eoun-Ebn-Ali wind farm in Tabriz, Iran. The operational data show that the turbine under study, with a classical PI controller, encounters high fluctuations when controlling the output power at its rated value. The turbine modeling is performed by deriving the non-linear dynamic equations of different subsystems. Then, the model parameters are identified such that the model response matches the actual response. In order to validate the proposed model, inputs to the actual wind turbine (wind speed, pitch angle and generator torque) are fed to the model in MATLAB as well as FAST tool, and the output powers are compared. In order to improve the control performance and alleviate fluctuations in the full-load region, considering the nonlinear and complex behavior of the system, a neuro-fuzzy controller is designed and simulated to control the pitch angle. In this controller, neural network is used to adjust the membership functions of the fuzzy controller. Simulation results of the designed neuro-fuzzy controller indicate the improved performance of the closed-loop system compared to the actual and simulated results from the classical PI controller.

Review History:
Received: 2018-11-20
Revised: 2019-06-08
Accepted: 2019-06-08
Available Online: 2019-12-01

Keywords:
Wind Turbine
FAST
Neuro Fuzzy Controller
Power Control

1. Introduction

Due to environmental, social and economic benefits, using wind energy is increasingly growing against other energy resources, particularly fossil fuel energies. Also, the significant advances in the wind turbines industry have accelerated the interest in the utilization of wind energy.

In the partial load region, where the wind speed is less than the rated value, extracting the maximum energy from wind is the goal of control. Many studies have been conducted to achieve this goal in this region. Moodi and Bustan.[1] proposed a novel T-S model with nonlinear consequent parts. Then, a robust H_∞ observer based fuzzy controller is designed to control the turbine using the estimated wind speed. Also, two networks are used to accurately model the aerodynamic curves. Velastimir et al. [2] utilized an advanced fuzzy controller for controlling wind turbine. In this paper, a model also analyzed and combined with a stochastic wind model for simulation purposes. Karabacak et al. [3] used a neural network structure to control a wind turbine. In this way, wind direction has been predicted and the wind turbine turns in this direction to extract the maximum energy of the wind. Yaakoubi et al. [4] presented the intelligent MPPT by using FLC (fuzzy logic control) due to its ability to cope with various problems. In the full-load region, extra loads have negative effects on different parts of the wind turbine. Therefore it reduces the turbine lifetime. Hence, in wind speeds above the rated value, the objective of the control system is to reserve the output power at its rated value, not to derive the maximum energy out of the wind [5-8].

The data from the Eoun-Ebn-Ali wind farm in Tabriz, Iran and the simulated results, demonstrate that the output power of these turbines have significant fluctuations and exceed the rated power frequently. This has negative effects on the turbine structure and can cause serious damages to different parts of the turbine. This is due to the poor performance of the classical controllers in controlling the blades pitch angle in the wind speeds higher than the rated value. Employing a deficient controller also increases vibrations and causes damages to mechanical parts of the turbine such as gearbox and blades. The controller should work as a damper in vibration modes in order to reduce the frequency loads and failure risk due to fatigue. Therefore, in this paper, an adaptive neuro-fuzzy controller has been designed in order to solve this problem and keep the output power at its rated value.

Different controllers from simple PI to advanced and intelligent controllers have been presented to adjust the pitch angle of the turbine blades and to limit the turbine power, in the full-load area. Hwas and Katebi [9] asserted a PI controller to control the pitch angle of wind turbine blades. This paper suggested two analytical and simulation-based methods to calculate the gains of a PI controller for a 5 MW

*Corresponding author's email: mo_taghizadeh@sbu.ac.ir

wind turbine. Sheikhan et al. [10] proposed an optimal fuzzy PI controller to capture the maximum power of the wind. A PI torque controller was proposed where its optimal gains were obtained from a particle swarm optimization algorithm and fuzzy logic theory. Rudion and Styczynski [11] modeled a wind turbine, then by controlling the pitch angle, kept the power at its rated value in the full-load region. Girsang et al. [12] designed a Multi-Input-Multi-Output (MIMO) Individual Pitch Controller (IPC) based on the knowledge of mitigated blade load at a yawed inflow condition. Lin et al. [13] proposed a Nonlinear PI (N-PI) controller for variable pitch wind turbines. The proposed N-PI did not require the accurate model and used only one set of PI parameters to provide a global optimal performance under wind speed changes.

Application of intelligent techniques to control wind turbines in the full-load region has also been considered in recent years. Guo et al. [14] proposed the pitch control algorithm of a wind turbine based on fuzzy and PID control. Lasheen and Elshafei [15] proposed a new fuzzy predictive algorithm for collective pitch control of large wind turbines. Habibi and Yousefi-Koma [16] used an adaptive fuzzy controller in the full-load operation. This has been done by two adaptive fuzzy controller units, including power and speed controllers. Adaptive rules used in the fuzzy controller were defined based on the errors of the generated power and angular velocity. Goyal et al. [17] considered power generation control in variable pitch wind turbines, using an adaptive fuzzy-PID controller. Shahnazi et al. [18] used an Radial Basis Function (RBF) neural network based PI pitch controller for a class of 5-MW wind turbines using particle swarm optimization algorithm. Yishuang and Meng [19] proposed the application of fuzzy PID controller to control the pitch angle of the wind turbine. They used a fuzzy controller to improve the system response time and reduce the overshoot.

Here, an adaptive neuro-fuzzy controller is designed to keep the output power at its rated value. In this controller, neural network is used to adjust the membership functions of the fuzzy controller. The neuro-fuzzy controller has a combination of fuzzy systems and neural networks advantages which uses fuzzy theory for presenting knowledge and employs the capability of learning from neural network to optimize the parameters [20-24]. The rest of the paper is organized as follows. In section 2, the wind turbine performance is discussed. In section 3, a model of the wind turbine is presented. Model validation with operational or actual data is done in section 4. The controller design is discussed in section 5 and simulation results are presented in section 6. Finally, the last section concludes the paper.

2. Wind turbine performance

The amount of energy that are absorbed by blades, depends on the area of rotor, air density, blades design and wind speed as follows.

$$P_{wind} = \frac{1}{2}\rho A V_{wind}^{3} \quad (1)$$

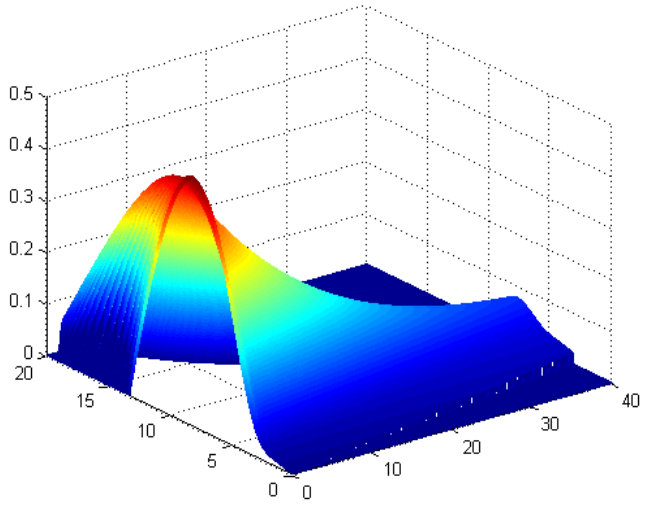

Fig. 1 3D diagram of $C_P(\lambda,\beta)$

$$P_a = C_P P_{wind} \quad (2)$$

When wind blows through the turbine blades with sufficient speed, blades move and cause the low speed shaft rotation. This shaft is connected to a gearbox to increase rotational speed. When high speed shaft reaches rated speed of generator, it drives the generator and produces electrical energy [25,26].

Typically, to explain the performance of wind turbines, non-dimensional characteristic curves can be used to indicate the actual performance of the wind turbine in different operating conditions. These curves are described as below.

2.1. $C_P - \lambda$ Performance curve

A common method to show the performance of wind turbines is the dimensionless curve of power coefficient-blade tip speed ratio. In variable speed wind turbines the maximum amount of power coefficient is approximately equal to 0.48 obtained at a blade tip speed ratio of 8.1[27-29]. In Fig. 1, this curve is depicted for a modern three-blade turbine.

2.2. Variable speed wind turbine performance regions

Variable speed wind turbine performance regions are shown in Fig. 2. Accordingly, wind turbines have been divided into three different regions.

Region 1: in this region, the turbine is not working because of the cost considerations.

Region 2 (low speed region): in this region, torque controller would be activated for control generator torque to extracting the maximum energy of the wind.

Region 3 (high speed region): when the wind speed reaches a rated value, pitch angle control will be activated in order to regulate the generator speed and power at their rated values [30].

3. Wind turbine modeling

Here, in modeling of the wind turbine the following assumptions have been considered.

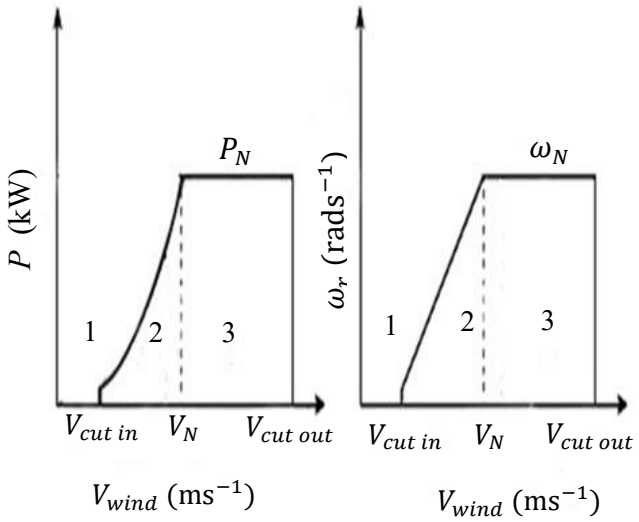

Fig. 2 wind turbines performance regions [20]

· Nonlinear modeling was considered and no linearization was performed in subsystems.

· Wind turbine blades were assumed to be perpendicular to the wind direction.

· The phenomenon of the wind shear was ignored.

In this paper, the variable speed wind turbine is divided into aerodynamic, drivetrain, electrical and pitch angle actuator subsystems.

3.1. Aerodynamic subsystem

Equation (3) shows the available power in the wind. It can be inferred from Eqn. (4) that power coefficient is a function of tip-speed ratio and pitch angle.

$$P_{wind} = \frac{1}{2}\rho A V_{wind}^3 \tag{3}$$

$$C_P(\lambda,\beta) = \frac{P_a}{P_{wind}} \tag{4}$$

The absorbed aerodynamic power by rotor can be calculated by Eqn. (5).

$$P_a = \frac{1}{2}\rho\pi R^2 C_P(\lambda,\beta) V_{wind}^3 \tag{5}$$

The relationship between power and aerodynamic torque is stated in Eqn. (6). The thrust force and the rotor torque can be obtained from Eqn. (7).

$$P_a = T_a \omega_r \tag{6}$$

$$T_a = \frac{\rho\pi R^3}{2} C_Q\left(\frac{\omega_r R}{V_{wind}},\beta\right) V_{wind}^2 \tag{7}$$

In Eqn. (8), torque coefficient C_Q can be obtained by Eqn. (8).

$$C_Q(\lambda,\beta) = \frac{C_P(\lambda,\beta)}{\lambda} \tag{8}$$

3.2. Mechanical subsystem

In order to model drivetrain, the dynamics of low speed shaft is modeled by Eqn. (9).

$$J_r \frac{d^2}{dt^2}\theta_r = T_a - T_1 - B_r \frac{d}{dt}\theta_r \tag{9}$$

Also, the dynamics of the high speed shaft is given by Eqn. (10).

$$J_{gen} \frac{d^2}{dt^2}\theta_{gen} = T_h - T_{gen} - B_{gen} \frac{d}{dt}\theta_{gen} \tag{10}$$

Then, gearbox is modeled as a gear ratio in Eqn. (11).

$$T_h = \frac{T_1}{N_{gear}} \tag{11}$$

Torsion of drivetrain subsystem is modeled by a torsional spring and damping coefficient.

$$T_1 = K_s \delta\theta + B\frac{d}{dt}\delta\theta \tag{12}$$

$$\delta\theta = \theta_r - \frac{\theta_{gen}}{N_{gear}} \tag{13}$$

$$\delta\omega = \omega_r - \frac{\omega_{gen}}{N_{gear}} \tag{14}$$

$$\frac{d}{dt}(\delta\theta) = \delta\omega = \omega_r - \frac{\omega_{gen}}{N_{gear}} \tag{15}$$

By replacing Eqn. (15) in (12), Eqn. (16) is obtained.

$$T_1 = K_s\delta\theta + B(\omega_r - \frac{\omega_{gen}}{N_{gear}}) \tag{16}$$

By replacing Eqn. (12) in (9), Eqn. (17) is obtained. Similarly, by replacing Eqn. (12) in (11), and then in (10), Eqn. (19) is gained. Finally, the dynamics of the drivetrain is defined by Eqns. (17) to (19).

$$J_r \frac{d}{dt}\omega_r = T_r - (k_s\delta\theta + B\delta\omega) \tag{17}$$

$$\delta\omega = \omega_r - \frac{\omega_{gen}}{N_{gear}} \tag{18}$$

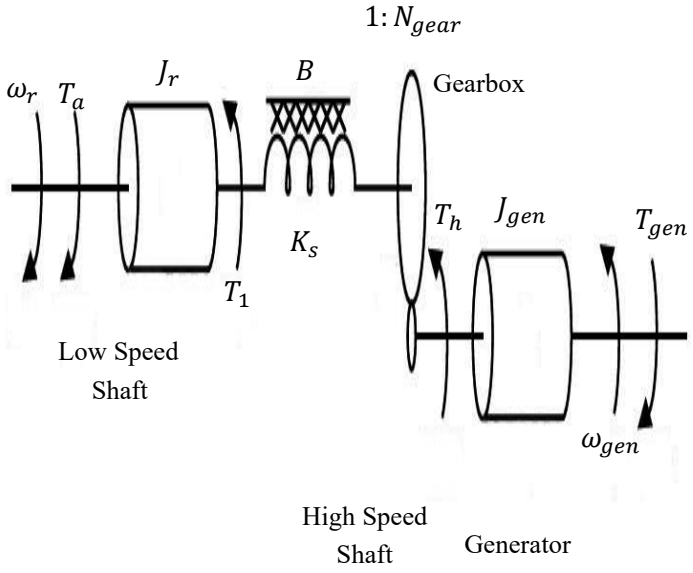

Fig. 3 Two mass model of wind turbine

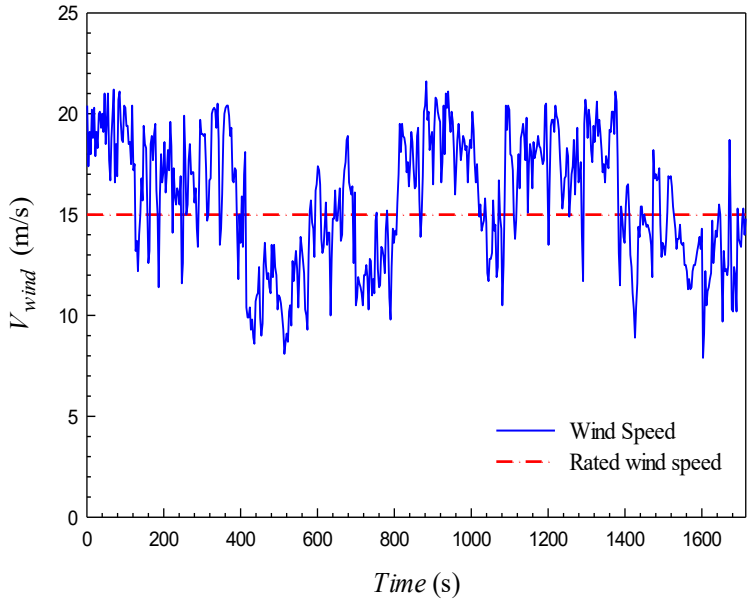

Fig. 4 Wind speed curve obtained from Eoun-Ebn-Ali wind power plant

$$J_{gen}\frac{d}{dt}\omega_{gen}=\left[\frac{1}{N_{gear}}\left(k_s\delta\theta+B\delta\omega\right)-T_{gen}\right] \tag{19}$$

Note that the viscous damping of low and high speed shafts are considered to be ignorable.

3.3. Electrical subsystems

The generator is investigated in this research, which is in the class of Wound Rotor Induction Generator (WRIG). The feature of this generator allows a variable slip. This generator reduces fluctuations in output power and torque by selecting optimum slip value. These generators have a variable external rotor resistance, which is controllable by slipping. Also, their stator is directly connected to the power network [5, 31, 32].

The output power of wind turbine can be obtained by Eqn. (20).

$$P_e=\eta_{gen}\omega_{gen}T_{gen} \tag{20}$$

Finally, the dynamics of the generator subsystem is modeled by Eqn. (21).

$$\dot{T}_{gen}=\frac{1}{\tau_{gen}}\left(T_{g,ref}-T_{gen}\right) \tag{21}$$

In this paper, two mass modeling is used to model wind turbine, which is demonstrated in Fig. 3 in details.

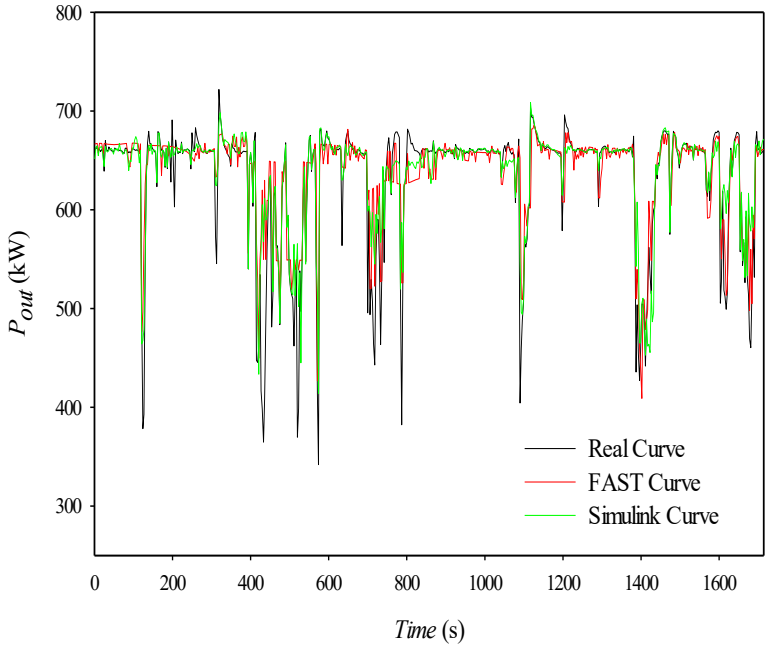

Fig. 5 Comparison of wind turbine output power in Simulink, FAST and real curves

3.4. Pitch actuator subsystem

The pitch actuator is a nonlinear servo system, which is compatible with the rotation of the whole or a part of blades. The control system uses the pitch actuator to prevent excessive loads on wind turbine structure in region 3 and keep the generator speed and power constant at their nominal values [7, 8, 33]. The dynamic behavior of the pitch actuator working in a linear range is given by

$$\dot{\beta} = -\frac{1}{\tau}\beta + \frac{1}{\tau}\beta_{opt} \tag{22}$$

4. Model validation with actual data and FAST tool

In this section, in order to validate the model in section 3, acquired actual data (wind speed, pitch angle, generator torque and output power) from Eoun-Ebn-Ali wind power plant are used. Curve depicted in Fig.4 , obtained from Vestas 660 kW wind turbine of Eoun-Ebn-Ali wind power plant.

In order to validate the proposed model, inputs to the real wind turbine (wind speed, pitch angle and generator torque) were considered as inputs to the model in MATLAB software as well as FAST tool, and the output powers were compared. The wind speed profile shown in Fig. 4 has been used to simulate the wind turbine performance. As shown in the Fig. 5, the output power of the real wind turbine, simulation results and FAST match with proper accuracy. The Root Mean Square Error (RMSE) between the actual data & Simulink output, and FAST & Simulink outputs are also calculated to be as follows.

RMSE of actual & Simulink data = 33.5418 kW

RMSE of FAST & Simulink data = 23.3247 kW

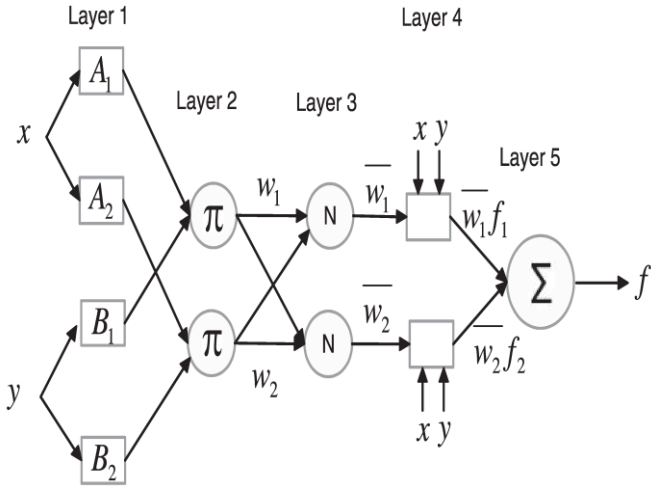

Fig. 6 ANFIS structure

5. Controller design

The Adaptive Neuro Fuzzy Inference System (ANFIS) is an artificial intelligent technique which creates a fuzzy inference system based on input and output information of the model. This system combines neural network and fuzzy system. ANFIS has the advantage of having both numerical and linguistic knowledge. ANFIS also utilizes the ability of ANN to classify data and identify patterns. Compared to the ANN, the ANFIS model is more explicit to the user and causes less memorization errors. Consequently, several advantages of the ANFIS exist, including its adaptation capability, nonlinear ability, and rapid learning capacity.

ANFIS can be used in a wide range of applications in modeling, decision making, and signal processing and control.

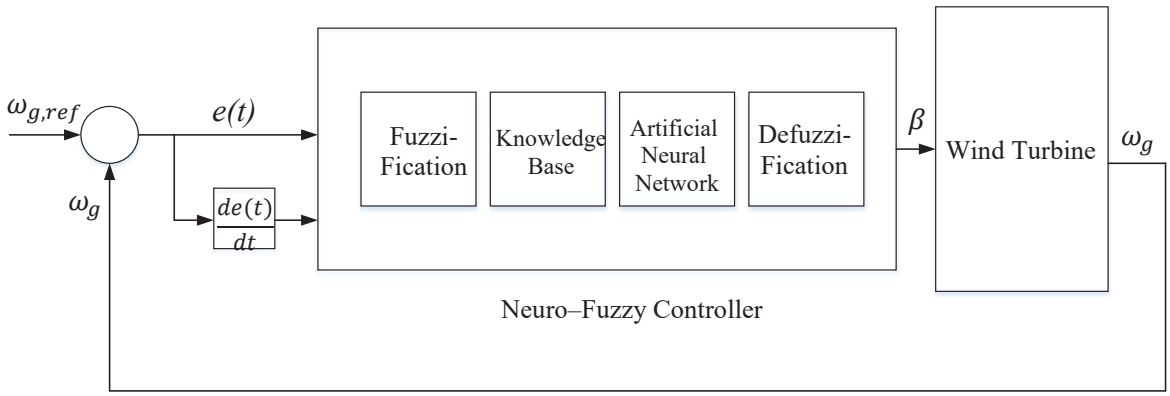

Fig. 7 block diagram of designed Neuro-Fuzzy Controller

This system is a class of adaptive networks which is a function of fuzzy inference system. The ANFIS algorithm combines neural network and fuzzy logic with 5 layers utilizing different node functions for learning and setting fuzzy inference system parameters. After learning, considering constant parameters, least square estimation method is used to update results [34-38]. The ANFIS system is a Sugeno type fuzzy model which is in the framework of an adaptive system in order to facilitate adaption and learning capabilities. Furthermore, this capability makes fuzzy controller more regulated and less dependent on expert knowledge.

As shown in Fig. 6, ANFIS has 5 layers. First and fourth layers are constructed from adaptive (settable) nodes and other three layers are constructed from constant (non-settable) nodes.

First layer (fuzzification): each node is adaptive in this layer. The output of this layer is the degree of membership of inputs which is stated as follows.

$$O_{ij}^{(1)} = \mu_{ij}(x), \qquad i = 1,\ldots,P \text{ and } j = 1,\ldots,n \tag{24}$$

$O_{ij}^{(1)}$ are outputs of each nodes in each layer which represent ith node in first layer, in proportion to input j. For instance, a bell membership function at first layer is obtained as follows.

$$\mu_{ij}(x_j) = \frac{1}{1+\left|\frac{x_j - c_{ij}}{a_{ij}}\right|^{2b_{ij}}} = \frac{1}{1+\left(\left(\frac{x_j - c_{ij}}{a_{ij}}\right)^2\right)^{b_{ij}}} \tag{25}$$

While parameters a_1, b_1 and c_1 are for first implication of first layer and the rest of similar parameters are for second to fourth implication of the first layer.

Second layer (rules layer): each node in this layer is a constant node and non-adaptive and shown with circle. The output of each layer is equal to the multiplication of its inputs which is demonstrated as follows.

Fig. 6 shows the equivalent structure of ANFIS for Sugeno model.

$$O_i^2 = w_i = \prod_k \mu_{ik} \qquad i = 1,\ldots,P \tag{26}$$

The output of each node (w_i) is the firing strength of each rule. In this layer, instead of multiplier operator, any fuzzy operator satisfying AND can be used.

Third layer: each node in this layer is constant. The output of ith node is equal to the ith firing strength divided by the total firing strength of all rules. Outputs of this layer are known as normalized firing strength.

$$O_i^3 = \overline{w}_i = \frac{w_i}{\sum_{k=1}^{P} w_k} \qquad i = 1,\ldots,P \tag{27}$$

Fourth layer (defuzzification layer): each node in this layer is adaptive. An output of this layer is consisted of multiplying later first order Sugeno fuzzy command in $\overline{w}_i$ coefficients.

$$O_i^4 = \overline{w}_i f_i = \overline{w}_i \left(\sum_{k=1}^{n} q_{ik} x_k + r_i\right) \qquad i = 1,\ldots,P \tag{28}$$

where, $\overline{w}_i$ is normalized firing strength that is obtained from third layer.

Fifth layer (summation neuron): the sole node in this layer is constant which the final output is from the summation of all outputs from fourth layer.

$$O^5 = y = \sum_i \overline{w}_i f_i = \frac{\sum_i w_i f_i}{\sum_i w_i} \qquad i = 1,\ldots,P \tag{29}$$

It is worth mentioning that the second, third and fifth layers are constant, while the first and fourth layers are adaptive. In other words, learning of the network is changing the parameters of these two layers to reach desired results. ANFIS structure is learned automatically by the least square

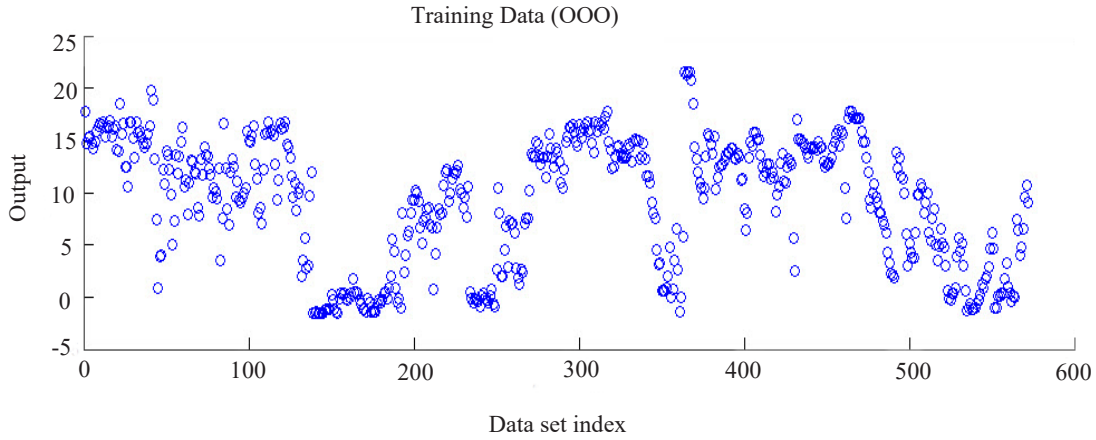

Fig. 8 training data obtained from fuzzy controller based on Sugeno model

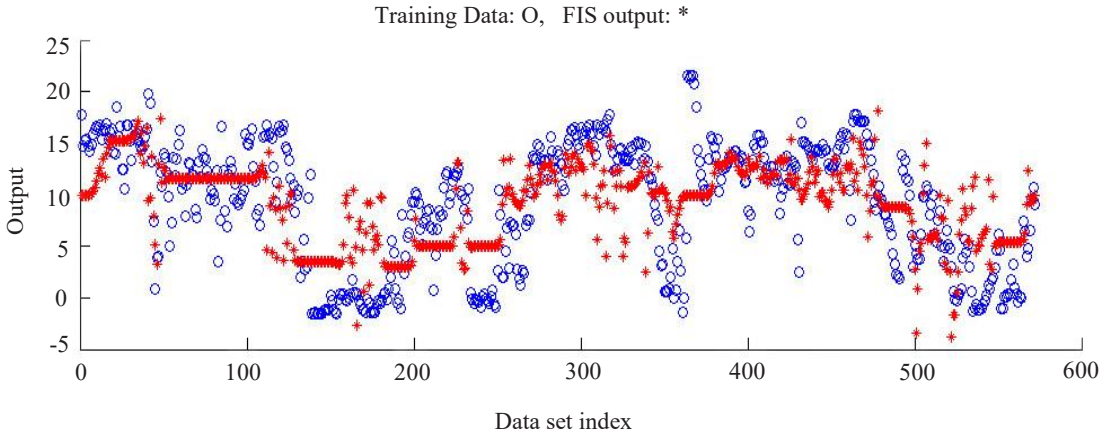

Fig. 9 comparison of training data with output of designed fuzzy controller in ANFIS editor

method and back propagation algorithm, or hybrid learning.

In this controller, Takagi-Sugeno model is used. In Fig. 7 a block diagram of the designed neuro-fuzzy controller is illustrated.

As shown in Fig. 7, the fuzzifier unit converts crisp information to linguistic variables which enter the rules block as inputs. A set of rules based on previous knowledge of system is written in rules block. Then, learning algorithm block for leaning neural network is placed to select a proper set of rules. For control signal this stage is critical. Finally, the output of the neural network is defuzzified and linguistic functions are converted to crisp form.

In this paper, a systematic approach for creating adaptive neuro-fuzzy controller is presented. This controller have self-organized and self-adaptive capabilities in accordance to its internal structure for learning control knowledge required to improve the performance of the control system.

If the wind speed is lower than nominal speed of wind turbine, the pitch angle is kept at its ideal value. When the wind speed exceeds the nominal value, controller becomes active and keeps the turbine power at its nominal value by changing the pitch angle to prevent excessive loads on turbine structure.

In this research, the generator speed error and its derivative are inputs and the pitch angle is output for this controller. These values are calculated by Eqns. (30) and (31), respectively.

$$e(t) = \omega_{gen} - \omega_{gen\_nom} \tag{30}$$

$$\frac{de(t)}{dt} = \frac{d(\omega_{gen} - \omega_{gen\_nom})}{dt} \tag{31}$$

When the output power of turbine is lower than nominal value, the error signal has a negative value and the pitch angle remains at its optimal value. When the output power exceeds the nominal value, the error signal becomes positive and the controller sets a new value for the pitch angle.

In this paper, the following steps were done for designing the neuro fuzzy controller to control the pitch angle:

· A fuzzy controller with Takashi-Sugeno model was designed.

· The designed controller was implemented on the model and simulated in MATLAB software.

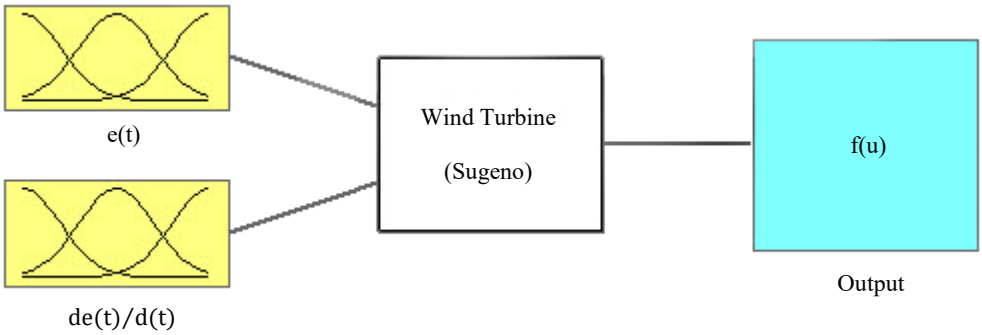

Fig. 10 inputs and outpu structure of designed controller

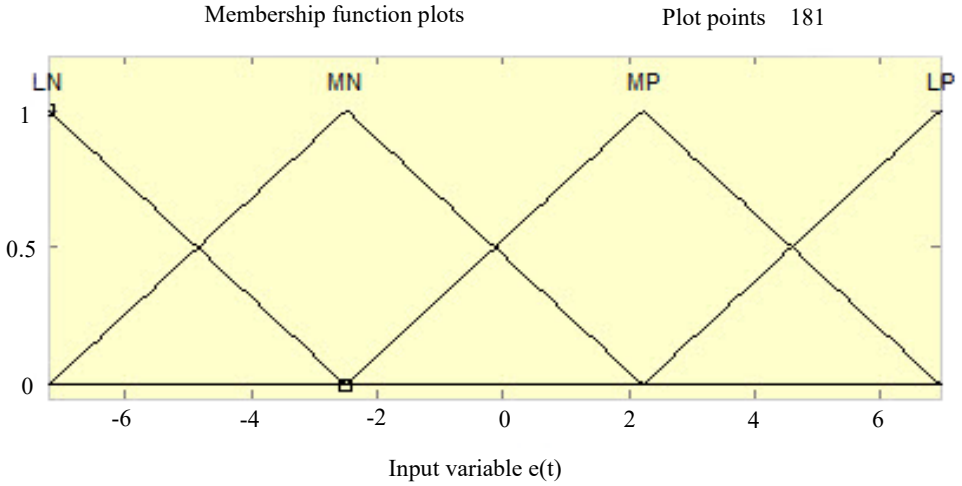

Fig. 11 membership functions of generator angular speed error

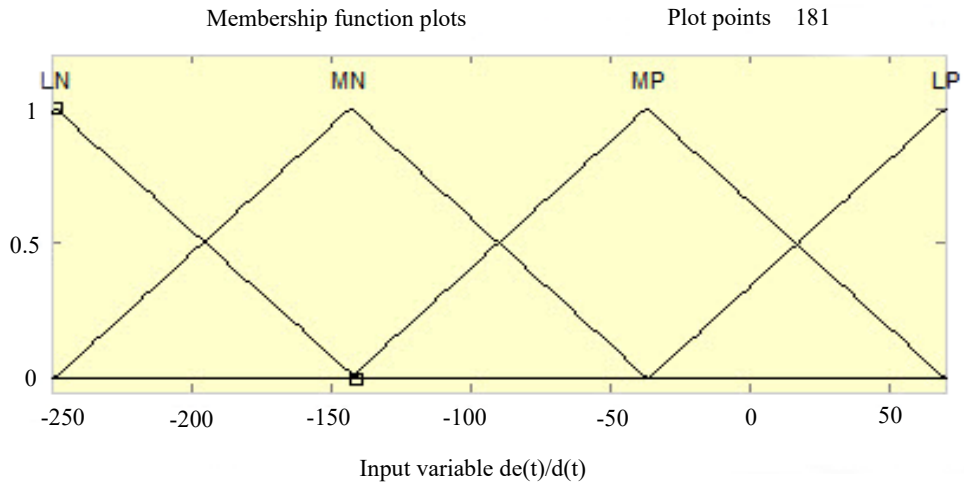

Fig. 12 membership functions of generator angular speed derivative error

· Inputs (generator angular speed error and its derivative) and output (blade pitch angle) of the simulation were acquired as training data.

· In the ANFIS editor, the training data was loaded as shown in Fig. 8.

· The designed fuzzy controller was loaded using FIS part in the ANFIS editor.

· Finally, using the ANFIS editor, the designed controller was trained. By adjusting the weight of neural network interfaces, the system parameters (membership functions, linguistic variables) were chosen to be close to the desired values by reducing the generator angular velocity error. Therefore, the controller performance was improved as shown in Fig. 9.

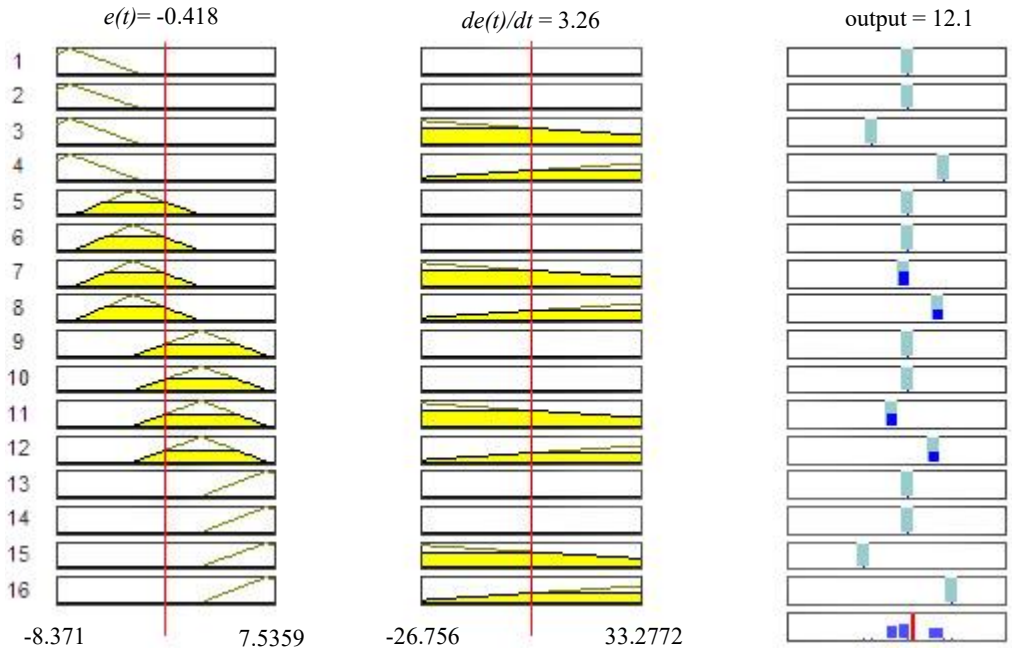

Fig. 13 avereage of rules used in designed neuro-fuzzy controller

Table 1. Numerical values of real and simulated wind turbines parameters

Item	Value	Units (SI)
Rotor diameter	47	(m)
Gear ratio	52.65	-
Rated Power	660	(kW)
Cut in wind speed	4	(ms^{-1})
Rated wind speed	15	(ms^{-1})
Cut out wind speed	25	(ms^{-1})
Air density	1.225	(kgm^{-3})
Rotor inertia	354000	(kgm^2)
Generator inertia	37.5	(kgm^2)
Shaft stiffness coefficient	293563	($Nm.rad^{-1}$)
Shaft damping coefficient	10363	($Nm.s.rad^{-1}$)
Tower height	40	(m)
Optimal pitch angle	0	(deg)
Optimal tip speed ratio	8.1	-
Generator time constant (τ)	15	(ms)
Generator communication delay	10	(ms)
Generator minimum load torque	0	(Nm)
Generator maximum load torque	3500	(Nm)
Pitch actuator time constant	35	(ms)
Pitch actuator communication delay	10	(ms)
Minimum rate of pitch actuator change	-10	(°/s)
Maximum rate of pitch actuator change	10	(°/s)
Minimum angle of pitch actuator	-10	(°)
Maximum angle of pitch actuator	90	(°)

In Fig. 10, the structure of the designed neuro-fuzzy controller has been shown.

In Figs. (11) and (12), membership functions of inputs to the designed controller have been shown. As shown in these Figures, triangular membership functions were used for inputs. Also, the range of variation for inputs has been determined. In these membership functions the following linguistic variables were used: Large Negative (LN), Medium Negative (MN), Medium Positive (MP), and Large Positive (LP).

Figure 13 represents the rules used in the neuro-fuzzy controller.

6. Simulation results

In this study, simulations are performed for a variable

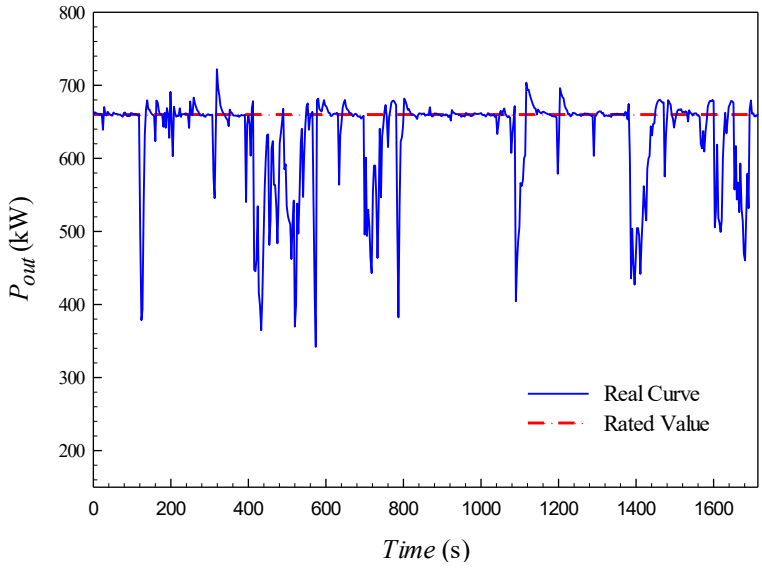

Fig. 14 Output power of the real wind turbine

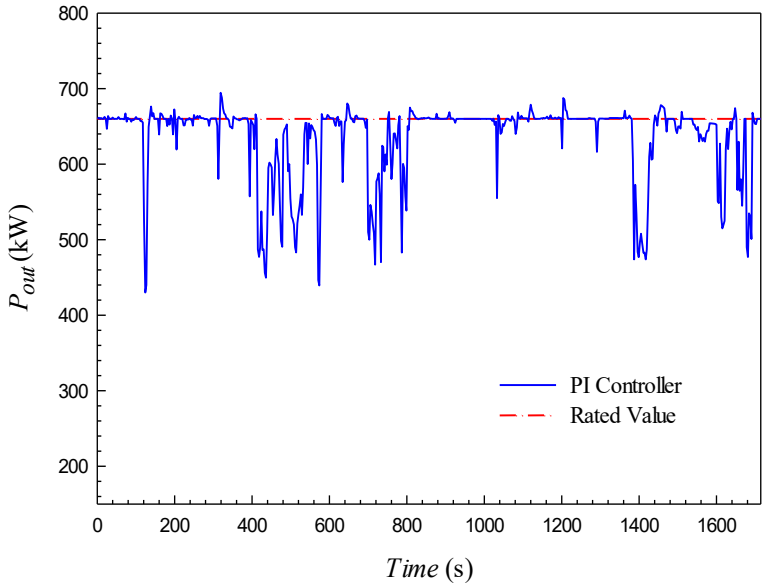

Fig. 15 Output power by using PI controller

speed wind turbine using MATLAB software (Simulink). The dimensions of the model are exactly similar to a Vestas 660kW wind turbine located in Eoun-Ebn-Ali wind farm in Tabriz. This turbine has three main components including rotor, tower and nacelle. Rotor has three blades and hub. Tower is a cylindrical pile, which holds the nacelle. Nacelle is a case where drivetrain is placed in it. The drivetrain system includes low-speed shaft, gearbox, high-speed shaft and the generator.

In the simulation, for the partial load or low speed region a classical PI controller has been used and we have focused on designing the controller for the full load or high speed region. Therefore, the designed neuro-fuzzy controller is implemented on the model in the full load region in MATLAB software. Then, the PI controller used in Vestas 660 kW wind is implemented on the model and simulated in MATLAB software. Finally, the results of the simulation with the neuro-fuzzy controller is compared in different diagrams with PI-controller and actual data obtained from Eoun-Ebn-Ali wind farm in Tabriz, Iran. Numerical values of real and simulated wind turbines parameters are listed in Table 1.

In order to simulate the wind turbine in this section, the wind speed curve shown in Fig. 4, has been used. As shown in Figs. 14 and 15, the output power in actual and simulated results of the classical controller have high fluctuations. Therefore, this causes negative effects on turbine structure and reduces the turbine lifetime.

However, according to the Fig. 16, using the designed neuro-fuzzy controller, fluctuations can be significantly reduced and the output power in the high speed region was

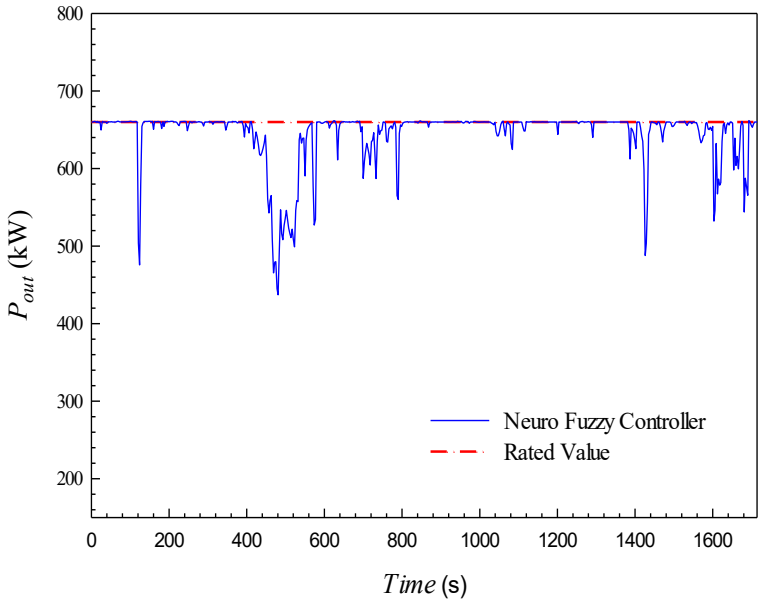

Fig. 16 Output power by using designed Neuro-Fuzzy controller

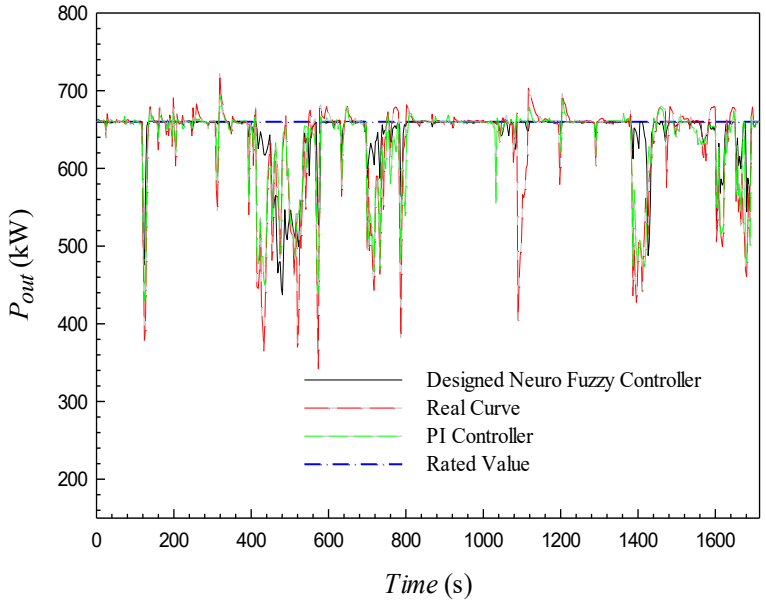

Fig. 17 Outputs power of designed neuro-fuzzy controller, PI controller and actual data

controlled at its rated value. Due to this favorable performance, structural loads on turbine can be reduced in wind speeds higher than the rated value.

Figure 17 shows the comparison of actual and simulated results of the classical PI controller with the designed neuro-fuzzy controller. As it can be seen, actual data and classical PI controller encounter high fluctuations around the rated power, while the designed Neuro-Fuzzy controller improved the control performance of the closed-loop system and alleviated fluctuations.

The Root Mean Square Error (RMSE) between the ANFIS & rated value, actual values & rated value and PI controller & rated value were calculated for the high speed region and listed in Table 2.

Table 2. Comparison of RMSE between the ANFIS & rated value, actual values & rated value and PI controller & rated value

RMSE	Rated Value (660 kW)
ANFIS Controller	0.359 kW
Actual Values	6.130 kW
PI Controller	3.927 kW

As it can be seen, the proposed ANFIS controller has reduced the RMSE compared to the classical PI controller and

Nomenclature

A	Area (m^2)
B	Shaft damping coefficient ($Nm.s.rad^{-1}$)
C_P	Power coefficient
F_T	Thrust force (N)
J_{gen}	Generator shaft moment of inertia (kgm^2)
J_r	Rotor shaft moment of inertia (kgm^2)
K_s	Shaft stiffness coefficient ($Nmrad^{-1}$)
N_{gear}	Gearbox gear ratio
P	Power (kW)
P_a	Aerodynamic power (kW)
T_a	Aerodynamic torque (Nm)
T_{gen}	Generator torque (Nm)
T_1	Applied torque to the low speed shaft (Nm)
T_h	Applied torque to the high speed shaft (Nm)
V_N	Rated wind speed (ms^{-1})
V_o	Wind speed proportion to the Rated power (ms^{-1})
V_{wind}	Wind speed (ms^{-1})
β	Pitch angle (deg)
β_{opt}	Optimum pitch angle (deg)
ε	Rotor angular speed error ($rads^{-1}$)
λ	Blade tip speed ratio
λ_{opt}	Optimum blade tip speed ratio
ω_r	Rotor angular velocity ($rads^{-1}$)
ω_{gen}	Generator angular velocity ($rads^{-1}$)

actual values, 90% and 94%, respectively.

7. Conclusions

In this research, a Vestas 660 kW wind turbine was modeled and the model was validated using operational data obtained from Eoun-Ebn-Ali wind farm in Tabriz-Iran. Moreover, a neuro-fuzzy controller was designed to control the output power at its nominal value in the full-load region. Actual data indicated that the turbine with a classical PI-controller, had high fluctuations around the rated output power, which exerted additional loads on the turbine structure. A neuro-fuzzy controller was designed to improve the control performance in the full-load region. The designed controller was then applied to the turbine model in Matlab/Simulink software. Simulation results showed that, the proposed ANFIS controller has significantly improved the control performance compared to the classical PI controller and real values.

References

[1] H. Moodi, D. Bustan, Wind turbine control using TS systems with nonlinear consequent parts, Energy, 172 (2019) 922-931.
[2] P.M. Živković, V.D. Nikolić, G.S. Ilić, Ž.M. Ćojbašić, I.T. Ćirić, Hybrid soft computing control strategies for improving the energy capture of a wind farm, Thermal Science, 16(suppl. 2) (2012) 483-491.
[3] K. Karabacak, N. Cetin, Artificial neural networks for controlling wind–PV power systems: A review, Renewable and Sustainable Energy Reviews, 29 (2014) 804-827.
[4] Yaakoubi, L. Amhaimar, K. Attari, M. Harrak, M. Halaoui, A. Asselman, Non-linear and intelligent maximum power point tracking strategies for small size wind turbines: Performance analysis and comparison, Energy Reports, 5 (2019) 545-554.
[5] Z. Civelek, Optimization of fuzzy logic (Takagi-Sugeno) blade pitch angle controller in wind turbines by genetic algorithm, Engineering Science and Technology, an International Journal, 23(1) (2020) 1-9.
[6] L. Romański, J. Bieniek, P. Komarnicki, M. Dębowski, J. Detyna, Estimation of operational parameters of the counter-rotating wind turbine with artificial neural networks, Archives of Civil and Mechanical Engineering, 17(4) (2017) 1019-1028.
[7] S. Bououden, M. Chadli, S. Filali, A. El Hajjaji, Fuzzy model based multivariable predictive control of a variable speed wind turbine: LMI approach, Renewable Energy, 37(1) (2012) 434-439.
[8] El Hajjaji, A. Khamlichi, Analysis of a RBF Neural Network Based Controller for Pitch Angle of Variable-Speed Wind Turbines, Procedia Engineering, 181 (2017) 552-559.
[9] Hwas, R. Katebi, Wind turbine control using PI pitch angle controller, IFAC Proceedings Volumes, 45(3) (2012) 241-246.
[10] M. Sheikhan, R. Shahnazi, A.N. Yousefi, An optimal fuzzy PI controller to capture the maximum power for variable-speed wind turbines, Neural Computing and Applications, 23(5) (2013) 1359-1368.
[11] K. Rudion, A. Orths, Z. Styczynski, Modelling of variable speed wind turbines with pitch control, in: Proceedings of The 2th International Conference on Critical Infrastructures, 2004, pp. 25-27.
[12] I.P. Girsang, J.S. Dhupia, Pitch controller for wind turbine load mitigation through consideration of yaw misalignment, Mechatronics, 32 (2015) 44-58.
[13] Y. Ren, L. Li, J. Brindley, L. Jiang, Nonlinear PI control for variable pitch wind turbine, Control Engineering Practice, 50 (2016) 84-94.
[14] R. Guo, J. Du, J. Wu, Y. Liu, The pitch control algorithm of wind turbine based on fuzzy control and PID control, Energy and Power Engineering, 5(3B) (2013) 6-10.
[15] Lasheen, A.L. Elshafei, Wind-turbine collective-pitch control via a fuzzy predictive algorithm, Renewable Energy, 87 (2016) 298-306.
[16] H. Hamed, A. K. Yousef, Wind Turbine Integrated Control during Full Load Operation, The 10th international Energy Conference (IEC), (2014).
[17] S. Goyal, M. Gaur, S. Bhandari, Power regulation of a wind turbine using adaptive fuzzy-PID pitch angle controller, International Journal of Recent Technology and Engineering, 2(3) (2013).
[18] Poultangari, R. Shahnazi, M. Sheikhan, RBF neural network based PI pitch controller for a class of 5-MW wind turbines using particle swarm optimization algorithm, ISA Transactions, 51(5) (2012) 641-648.
[19] Y. Qi, Q. Meng, The Application of Fuzzy PID Control in Pitch Wind Turbine, Energy Procedia, 16 (2012) 1635-1641.
[20] A. I. Yousif, Design and Simulation of Anfis Controller for Virtual-Reality-Built Manipulator. Recent Advances in Theory and Applications, Intech, (2012)..
[21] E. Assareh, M. Biglari, A novel approach to capture the maximum power from variable speed wind turbines using PI controller, RBF neural network and GSA evolutionary algorithm, Renewable and Sustainable Energy Reviews, 51 (2015) 1023-1037.
[22] F. Jaramillo-Lopez, G. Kenne, F. Lamnabhi-Lagarrigue, A novel online training neural network-based algorithm for wind speed estimation and adaptive control of PMSG wind turbine system for maximum power extraction, Renewable Energy, 86 (2016) 38-48.
[23] Medjber, A. Guessoum, H. Belmili, A. Mellit, New neural network and fuzzy logic controllers to monitor maximum power for wind energy conversion system, Energy, 106 (2016) 137-146.
[24] H. Simon. Neural Networks and Learning Machines, Pearson Prentice Hall, (2009).

[25] H. Jiang, Y. Li, Z. Cheng, Performances of ideal wind turbine, Renewable Energy, 83 (2015) 658-662.
[26] Pintea, H. Wang, N. Christov, P. Borne, D. Popescu, A. Badea, Optimal control of variable speed wind turbines, in: 2011 19th Mediterranean Conference on Control & Automation (MED), (2011), 838-843.
[27] V. Fazlollahi, M. Taghizadeh, F. A Shirazi, ANFIS modeling and validation of a variable speed wind turbine based on actual data, Energy Equipment and Systems, 7(3) (2019) 249-262.
[28] F. D. Bianchi, H. D. Battista, R. J. Mantz, Wind Turbine Control Systems Principles, Modelling and Gain Scheduling Design .Springer: La Plata, (2006)
[29] A.B. Asghar, X. Liu, Estimation of wind turbine power coefficient by adaptive neuro-fuzzy methodology, Neurocomputing, 238 (2017) 227-233.
[30] T. Burton, D. Sharpe, N. Jenkins, E. Bossanyi. Wind Energy Handbook. Wiley: West Sussex, (2001) 176-177.
[31] T. Sandhya, K.S. Chandan, Control and operation of Opti-slip induction generator in wind farms, in: 2011 International Conference on Computer, Communication and Electrical Technology (ICCCET), (2011) 450-454.
[32] A.R. Tiwari, A.J. Shewale, A. Gagangras, N.M. Lokhande, Comparison of various wind turbine generators, Multidiscplinary Journal of Research in Engineering and Technalogy, 1(2) (2014) 129-135.
[33] R. Guo, J. Du, J. Wu, Y. Liu, The pitch control algorithm of wind turbine based on fuzzy control and PID control, Energy and Power Engineering, 5(3B) (2013) 6-10.
[34] R. Isanta Navarro, Study of a Neural Network-based System for Stability Augmentation of an Airplane, Annex1, Introduction to Neural Networks and Adaptive Neuro-Fuzzy Inference Systems (ANFIS), Technical Report, Catalunya, (2013).
[35] F. Golnary, H. Moradi, Dynamic modelling and design of various robust sliding mode controls for the wind turbine with estimation of wind speed, Applied Mathematical Modelling, 65 (2019) 566-585.
[36] A.B. Asghar, X. Liu, Adaptive neuro-fuzzy algorithm to estimate effective wind speed and optimal rotor speed for variable-speed wind turbine, Neurocomputing, 272 (2018) 495-504.
[37] M. Morshedizadeh, M. Kordestani, R. Carriveau, D.S.-K. Ting, M. Saif, Application of imputation techniques and Adaptive Neuro-Fuzzy Inference System to predict wind turbine power production, Energy, 138 (2017) 394-404.
[38] P. Srisaeng, G.S. Baxter, G. Wild, An adaptive neuro-fuzzy inference system for forecasting Australia's domestic low cost carrier passenger demand, Aviation, 19(3) (2015) 150-163.

HOW TO CITE THIS ARTICLE

V. Fazlollahi, M. Taghizadeh, F.A. Shirazi, Meng and Neuro-fuzzy Controller Design of a Wind Turbine in Full-load Region Based on Operational Data, AUT J. Model. Simul., 51(2) (2019) 139-152.

DOI: 10.22060/miscj.2019.15315.5130